H. Moki[1*], K. Yanagita[2], K. Kondo[2], and T. Kuwae[1]

[1] Coastal and Estuarine Environment Research Group, Port and Airport Research Institute, National Institute of Maritime, Port and Aviation Technology, 3-1-1 Nagase, Yokosuka 239-0826, Japan.

[2] Science and Technology Co., Ltd., 4-12-44 Shibaura, Minato-ku, Tokyo, 108-0023, Japan.

Corresponding author: Hirotada Moki (moki-hi@p.mpat.go.jp)

Key Points:

- The current distribution of major shallow water ecosystems excluding coral can be sustained or increase by 2100.
- Seagrass meadows are projected to increase by up to 11% by 2100 because of increased photosynthetic active radiation depth.
- The landward shift of tidal marshes and mangroves with sea-level rise is important.

Abstract

The global area and distribution of shallow water ecosystems (SWEs), and their projected responses to climate change, are fundamental for evaluating future changes in their ecosystem functions, including biodiversity and climate change mitigation and adaptation. Whereas previous studies have focused on a few SWEs, we modelled the global distribution of all major SWEs (seagrass meadows, macroalgal beds, tidal marshes, mangroves, and coral habitats) from current conditions (1986−2005) to 2100 under the RCP2.6 and RCP8.5 emission scenarios. Our projections show that global coral habitat shrank by as much as 75% by 2100 with warmer ocean temperatures, but macroalgal beds, tidal marshes, and mangroves remained about the same because photosynthetic active radiation (PAR) depth did not vary greatly (macroalgal beds) and the shrinkage caused by sea-level rise was offset by other areas of expansion (tidal marshes and mangroves). Seagrass meadows were projected to increase by up to 11 % by 2100 because of the increased PAR depth. If the landward shift of tidal marshes and mangroves relative to sea-level rise was restricted by assuming coastal development and land use, the SWEs shrank by 91.9% (tidal marshes) and 74.3% (mangroves) by 2100. Countermeasures may be necessary for coastal defense in the future; these include considering the best mix of SWEs and coastal hard infrastructure because the significant shrinkage in coral habitat could decrease wave energy. However, if appropriate coastal management is achieved, the other four SWEs, which relatively have high CO_2 absorption rates, can help mitigate the climate change influences.

Plain Language Summary

Because shallow water ecosystems (seagrasses, macroalgae, tidal marshes, mangroves and coral reefs) play important roles in absorbing CO_2 and decreasing

wave energy, it is important to project their future distribution in the face of climate change. We used numerical models to project the global distribution of these ecosystems through 2100. Our results show that global coral reef shrank by as much as 75% with warmer ocean temperatures, but seagrasses increased by up to 11% because of the increased depth of active photosynthesis. Other ecosystem areas remained about same because the depth of active photosynthesis did not vary greatly (macroalgae) or the shrinkage caused by sea-level rise was offset by a landward shift (tidal marshes and mangroves). However, if the landward shift is restricted by coastal development, tidal marshes and mangroves could shrink by 91.9% and 74.3%, respectively. Coastal hard infrastructure and other countermeasures may be necessary for coastal defense in the future, particularly in coral reefs. If appropriate coastal management is achieved, non-coral shallow water ecosystems, which have relatively high CO_2 absorption rates, can help mitigate the influences of future climate change.

1 Introduction

Although SWEs account for only 0.2% of the world's total ocean area, they account for 73 79% of the total carbon sequestration rate of the global ocean (Duarte et al., 2005; Nelleman et al., 2009; Hori et al., 2019). These ecosystems can be expected to have important effects in mitigating climate change by storing blue carbon. In addition, SWEs offer promise with respect to climate change adaptation against sea-level rise (Kirwan and Mudd, 2012, Duarte et al., 2013). Although green infrastructure including SWEs may be less effective than grey infrastructure in terms of disaster prevention and mitigation, SWEs have the benefits of natural resilience and low maintenance costs (Kay and Wilderspin, 2002). Furthermore, these ecosystems, when well maintained or restored, provide ecosystem services that help enhance water quality, food provision, biodiversity strategies, fisheries, recreational and cultural benefits (Haight et al., 2019; Duarte et al., 2020).

The distribution and area of SWEs will be affected by climate change; however, projections of the future distribution and area of SWEs are under debate and not well constrained. Coastal wetlands, including tidal marshes and mangroves, have been projected to shrink by 20 90% as a result of sea-level rise (IPCC, 2019). However, this estimate has several issues. One is that sea-level rise by 2100 is projected as a uniform rise of 1 m across the globe (Blankespoor et al., 2014); other more serious concerns are that this amount of sea-level rise is greater than the amount under the Representative Concentration Pathway 8.5 (RCP8.5) scenario (IPCC, 2019) and that the estimate does not take into account the expansion of ecosystem areas due to sea-level displacement (Spencer et al., 2016). By one estimate, tidal marshes and mangroves will be sustained (Kirwan et al., 2010; Lovelock et al., 2015) or expand by up to 60% (Schuerch et al., 2019) over the present levels due to increasing deposition of suspended matter. However, hard coastal structures and land use are extremely important factors. A previous study predicted that the distribution of tidal marshes and mangroves shrunk considerably when SWEs cannot shift landward because of

hard coastal structures (Kirwan et al., 2010). A prediction of coral habitats based on temperature changes has argued that the current areas of coral will be almost completely lost by 2100 (Frieler et al., 2013), but it does not take into account habitat shift or relocation of corals to new areas with suitable water temperatures. Another study of coral habitats has projected 75% losses due to the shift to deeper sea beds with accompanying temperature changes, but it does not take into account latitudinal shifts (Jorda et al., 2020). Seagrass meadows and macroalgal beds have been also projected to shrink by 8.6% and 20.6% by 2100, respectively, if no changes in the photic layer occur. Thus, previous studies have not adequately considered the adaptation of SWEs to climate change. Additionally, because all SWEs can play an important role in climate change mitigation and adaptation, integrated predictions are necessary; however, previous studies have focused on at most three types of SWEs (Jorda et al., 2020; Lovelock et al., 2020).

In this study, we projected the global distribution and area of the five most important SWEs (seagrass meadows, macroalgal beds, tidal marshes, mangroves, and coral habitats) from their current state to 2100, by integrating topographic data and the current global distribution of SWEs and using a global climate model as an external forcing under two emissions scenarios, RCP2.6 and RCP8.5. Furthermore, we predicted the distribution of tidal marshes and mangroves when SWEs cannot shift landward with sea-level rise because of hard coastal structures and land use.

2 Methods

2.1 Computational region

To simplify computation while reflecting the topography and ecosystem distribution specific to given regions, we divided and categorized global coastlines into computational domains. Global coastlines have been classified on the basis of coastal topographic entities, types such as deltas or fjords, etc (Durr et al., 2011). Based on these global coastline types, adjacent line segments shorter than 1,000 km that were of the same type were merged, yielding 198 computational areas (the mean coastline length was about 2,000 km) as shown in Figure S1. Because SWEs have the potential to expand or shift not only in the cross-shore direction but also in the coastline direction, the entire length of each segment, which was divided based on the coastline type, was applied to the computational domain to account for its potential in this study.

2.2 Geographical data

Topographic data for land and sea were derived from the Shuttle Radar Topography Mission 15 PLUS (SRTM-15PLUS) dataset (WebGIS: http://www.webgis.com/srtm3.html). The spatial resolution of this dataset is about 450 m. Topography in the landward direction was incorporated to an elevation of up to 50 m to ensure adequate coverage when the SWEs expand in the future. Bathymetry was incorporated to 100 m depth to encompass the depth range from the maximum high-tide surface to the euphotic layer (Figure S2). The elevation data

were averaged along the shoreline direction for each of the 198 computational areas ArcGIS software (ESRI, Inc.) to generate hypsometric curves in the offshore direction with a horizontal resolution of 100 m (Figure S3). The zero elevation point, which is the boundary between sea and land, was obtained from Open Street Map Data (https://osmdata.openstreetmap.de/).

2.3 Distribution of SWEs

The five SWEs we focused on were seagrass meadows, macroalgal beds, tidal marshes, mangroves and coral habitats. As with the topographic data, the SWE area was compiled in each of the 198 areas classified in "Computational region" (Figure S1). These data were obtained from UNEP-WCMC except for macroalgal beds (Figure S4 and Table S1). Because there are no available data for the global distribution of macroalgal beds, we adopted the total global area reported in the literature (Krause-Jensen and Duarte, 2016). Because macroalgae are nearly ubiquitous in coastal areas (Assis et al., 2020), we assumed that all 198 computational regions are habitable areas for macroalgae. Macroalgal beds constitute the largest area among the SWEs (Table S1).

2.4 Regulating factors for SWE projections

When projecting changes in the distribution and extent of SWEs due to climate change, we considered the following regulating factors: water temperature for coral habitats, chlorophyll concentration and sea-level change for seagrass meadows and macroalgal beds, and sea-level change for tidal marshes and mangroves. The IPCC special report on the ocean and cryosphere in a changing climate (IPCC, 2019) estimated a maximum rise of 110 cm in sea level by 2100. The major global climate models (GCMs) used in climate prediction are summarized in the Coupled Model Intercomparison Project phase 5 (CMIP5) (Taylor et al., 2012). For this study, we used results from the GFDL-ESM2M model (Dunne et al., 2012), which has a relatively rich set of marine chemical and physical variables, as the regulating factors for calculating changes in SWE extents. For the Representative Concentration Pathways (RCP) scenarios, we adopted RCP2.6 and RCP8.5. As described in the next section, this study performed calculations in the present state and the future. The GCM's output data from historical experiments were used as regulating factors in calculations of the present state, and the variables in the RCP scenarios were used for the future projections. For applying the GCM results, we extracted the data adjacent to the land area of each of the 198 computational areas, and averaged these data for use in our projections of SWE change.

2.5 Computational term

The period for the calculation of present conditions is 1986–2005, and the period for predicted conditions is 2031–2100. Sea-level change is applied as regulating factor for calculating changes in the extent of seagrass meadows, macroalgal beds, tidal marshes, and mangroves, but the results calculated by the GCM are defined as "sea level height from geoid layer" (ZOS) and "thermosteric sea level change" (ZOSTOGA). Therefore, we established ZOS+ZOSTOGA aver-

aged over the present period as the basis and adopted the difference between the present and each month of the future period as sea-level change. Although the future predictions are performed on a monthly basis, it is plausible that the calculation results would be biased when particular months or portions of the year are used for comparison. Therefore, we averaged the calculated results for the present state over 20 years and those for the future predictions over 10 years, respectively, and compared these averages to reduce the bias (Table S2).

2.6 Projection of seagrass meadows and macroalgal beds

The effect of light intensity is maximal on primary production in benthic ecosystems, and it also has an effect on seagrass meadows and macroalgal beds (Dennison, 1987; Duarte 1991; Delesalle et al., 1993; Borum and Sand-Jensen, 1996; Nielsen et al., 2002), but it has been reported that photoinhibition may not affect the growth of seagrasses (Lee et al., 2007). They do, however, require a minimum quantity of light for growth (Duarte, 1991; Gattuso et al., 2006), indicating that low light levels are a greater constraint on seagrass growth than high light levels. Although macroalgae has been reported to exhibit photoinhibition (Hanelt and Figueroa, 2012), in the absence of relevant data for the diverse range of macroalgal species, we assumed that macroalgae, like seagrasses, are not subject to photoinhibition. In this study, we calculated the maximum water depth at which sufficient light exists for the growth of seagrasses and macroalgae with the following equation proposed in previous studies (Duarte, 1991; Gattuso et al., 2006; Morel 1998):

$$\mathrm{LN}\,(Z_c) = \alpha - \beta \bullet LN\,(K_{\mathrm{PAR}}) \quad (1)$$

$$K_{\mathrm{PAR}} = 0.121 \bullet \mathrm{Chl}^{0.428} \quad (2)$$

the values and coefficients for which are defined in Table S3. The light attenuation coefficient (K_{PAR}) is calculated by using the chlorophyll-a concentration (Chl) as a proxy for light attenuation, and the photosynthetic active radiation (PAR) depth (Z_c) is calculated from K_{PAR}. The distribution width (L) is estimated (Figure S5) from Z_c and the hypsometric curve for each computational area (Figure S3).The current distribution width (L_p) is estimated from current data, and the future distribution width (L_f) is estimated by recalculating Z_c^f from future chlorophyll-a concentrations and sea-level change. In this study, the future area was estimated by multiplying the ratio L_f/L_p by the current habitat area (E_p). The areal change in seagrass meadows was estimated in each of the 198 computational areas and summed as the future global distribution area:

$$E_f^{\mathrm{sg}} = \sum_{n=1}^{L_{\mathrm{nmax}}} E_{\mathrm{psg}}^n \bullet \frac{L_{\mathrm{fsg}}^n}{L_{\mathrm{psg}}^n} \quad (3)$$

For macroalgal beds, lacking data specific to the computational areas, the future global distribution area was estimated by

$$E_f^{\mathrm{SW}} = E_p^{\mathrm{SW}} \bullet \sum_{n=1}^{L_{\mathrm{nmax}}} \frac{L_{\mathrm{fSW}}^n}{L_{\mathrm{pSW}}^n} \quad (4)$$

Terms in these equations are defined in Table S3.

In this study, the PAR depth was the governing environmental parameter for the change in SWE area. PAR depth depends on changes in the chlorophyll-a concentration. Moreover, the chlorophyll-a concentration applied in this study depends on offshore environmental changes because it is the result of GFDL-ESM2M, which is one of the GCMs used. Coastal chlorophyll-a concentration can be influenced by anthropogenic effects from land, but when the global coasts are divided into 198 segments, such as in this study, the ratio of region open to offshore increases. Because the effects of nutrients from offshore inputs are greater than those from anthropogenic inputs for ecosystems open to offshore (Jickells, 1998; Arin et al., 2013), we applied the chlorophyll-a concentration from the GCM as the input parameter. Although other parameters are known to be influential, these were ignored for lack of firm constraints.

Ranges of water temperatures that are optimal or sufficient for the growth of seagrasses and macroalgae have been reported, but these differ among species, and thus, if we consider multiple species, seagrasses and macroalgae can inhabit a wide range of shallow water areas (Eggert, 2012; Lee et al., 2007). In general, species in mid to high latitudes favor lower water temperatures, and species in low latitudes favor higher temperatures. If water temperatures in mid to high latitudes increase, ecosystems based on currently dominant species may disappear while dominant species from lower latitudes may expand to higher latitudes (Takao et al., 2015). Thus, the adaptability of these SWEs to changes in water temperature may be greater than the adaptability of specific species. Nutrients are also a limiting factor for the growth of seagrass and macroalgae. However, because the intake rate of nutrients is influenced by light intensity in the first place, light intensity is more important (Harrison and Hurd, 2001). In addition, the nutrients in pore water affect the growth of seagrasses (Lee et al., 2007), although the global distribution of nutrient concentration and future changes in it are poorly understood. Therefore, nutrients are not accounted for in this study.

Because other environmental conditions (such as salinity, precipitation and bottom sediment) are not known in detail in areas adjoining but not presently containing (seagrass meadows, macroalgal beds, tidal marshes, and mangroves), we did not consider the possible expansion of these SWEs into new areas, but we did consider changes of their current distribution areas in the offshore and onshore directions.

2.7 Projection of tidal marshes and mangroves

Tidal marshes and mangroves occupy the intertidal area. In this study, we assumed that tidal marshes and mangroves are distributed from MSL to mean high water spring tide (MHWS) (Figure S6). Because sea-level change markedly influences in changes in the distribution of tidal marshes and mangroves (Nuttle et al., 1997; Phan et all., 2015), we used topographic and sea-level data to calculate the changes in the distribution width of each ecosystem after sea-level change. We then estimated the future area by multiplying the ratio of future change by the current ecosystem area. We summed the 198 computational areas

to determine the total future area after estimating the area of tidal marshes from

$$E_f^{\mathrm{sal}} = \sum_{n=1}^{L_{\mathrm{nmax}}} E_{\mathrm{psal}}^n \bullet \frac{L_{\mathrm{fsal}}^n}{L_{\mathrm{psal}}^n} \quad (5)$$

and the area mangroves from

$$E_f^{\mathrm{mg}} = \sum_{n=1}^{L_{\mathrm{nmax}}} E_{\mathrm{pmg}}^n \bullet \frac{L_{\mathrm{fmg}}^n}{L_{\mathrm{pmg}}^n} \quad (6)$$

The terms in these equations are defined in Table S4. We extracted tidal data for each month from 1986 to 2005 from the TOPEX/Poseidon dataset (TPXO8-ATLAS) (Egbert and Erofeeva, 2002), and the averaged data were applied to the projection.

2.8 Projection of coral habitats

For coral habitats, high water temperature is fatal (Hoegh-Guldberg and Smith, 1989). Previous studies have reported that coral bleaching occurs when SST on the warmest month of the year exceeds above 30°C (Kayanne et al., 1999; Guinotte et al., 2003; Yara et al., 2012). It has also been reported that coral habitats can expand into previously unsuitable areas when SSTs for the annual coldest and warmest months are above 18°C and below 30°C, respectively (Kleypas et al., 1999). In this study, we used these constraints when calculating the changes in coral habitat distribution from the present to the future. We assumed that coral bleaching eliminated coral habitat when SST in the warmest month exceeds 30°C for more than five years in a calendar decade (2021 2030, 2031 2040, etc.). We also excluded areas from coral expansion in which SST on the annual coldest month is below 18°C. The area of habitat expansion was determined by multiplying the area in which coral habitats expand by the global average proportion of present coral habitat in the area of coastal shallow waters. Areas where there are no coral habitats despite having the appropriate SST range were excluded because other environmental factors may have hindered the establishment of corals.

Although high water temperature is thought to be the main cause of coral loss, other factors have been cited such as acidification and light transmittance changes in seawater. A previous study has found that the effect of acidification was negligible (Frieler et al., 2013). To evaluate the effect of changes in light transmittance in sea water, the light demands for photosynthesis of diverse zooxanthellae are necessary, but they are poorly understood. Therefore, SST was the only environmental factor we considered for calculating the change of coral habitat distribution in this study.

2.9 Sedimentation rate

The effects of particulate matter sedimentation are more pronounced in SWEs where the sediment consists of sand and mud (seagrass beds, tidal marshes and mangroves). Specifically, bottom friction and the drag force of submerged aquatic vegetation increase the rate of sediment accumulation (Ward et al., 1984; Struve et al., 2003; Bouma et al., 2007), which can offset the effect of sea-level

rise. In this study, we assumed a sedimentation rate of 1.68×10^{-4} m/month for seagrass meadows, based on Duarte et al. (2013), and held it constant throughout the computational period. Sedimentation was not considered for tidal marshes and mangroves because the average shoreline length in each computational area is approximately 2,000 km, and the average hypsometric curve includes relatively steep terrain outside the gently sloping intertidal area; thus, we considered future changes in sedimentation in these areas to be negligible because of the intertidal zone being absorbed into the spatial resolution in the coast-offshore direction (>100 m).

2.10 Interaction between environmental variables and feedbacks and tipping point

In seagrass meadows, transparency changes with topography changes that are induced by sedimentation, and seagrass meadows shifted landward also changes the region of sedimentation. For the other SWEs, because only one environmental factor is applied as described above, interaction and feedback cannot be considered. Furthermore, multiple SWEs can be included in one region, but each SWE is highly independent because they do not necessarily overlap at the same point in a region along a coastline of few thousand km and are often scattered. Therefore, interaction and feedback between the SWEs are not taken into account in this study.

2.11 Subsidence

This study estimates the effects of subsidence on the distribution of tidal marshes and mangroves. Subsidence in several deltas (Syvitski et al., 2009) was assigned to 7 tidal marsh regions and 12 mangrove regions (Tables S5 and S6). Furthermore, relative subsidence was accounted for by adding it to sea-level rise following the method of Schuerch et al. (2019). Future global subsidence is unknown, so we applied the present subsidence.

3 Results and discussion

Our results showed that the total area of SWEs shrinks by only 1.4 to 1.5% by 2100 and that all SWEs can have the potential to adapt to climate change (Figure 1a). In particular, the distribution areas of four SWEs (seagrass meadows, macroalgal beds, tidal marshes, and mangroves) did not notably shrink in the RCP2.6 scenario (Figure 1b 1e). In the RCP8.5 scenario, only seagrass meadows expanded (by 11%) over present state (Figure 1b). However, coral habitats shrank appreciably by 2100 (by 25% in RCP2.6 and by 74% in RCP8.5) (Figure 1f). The proportions of each of the five SWEs showed little change from the present to 2100 in both RCP scenarios (Table 1): macroalgal beds varied from 84.9% to 85.8%, followed by seagrass meadows (7.5 8.4%), mangroves (3.7%), coral habitats (0.7 2.6%) and tidal marshes (1.3%).

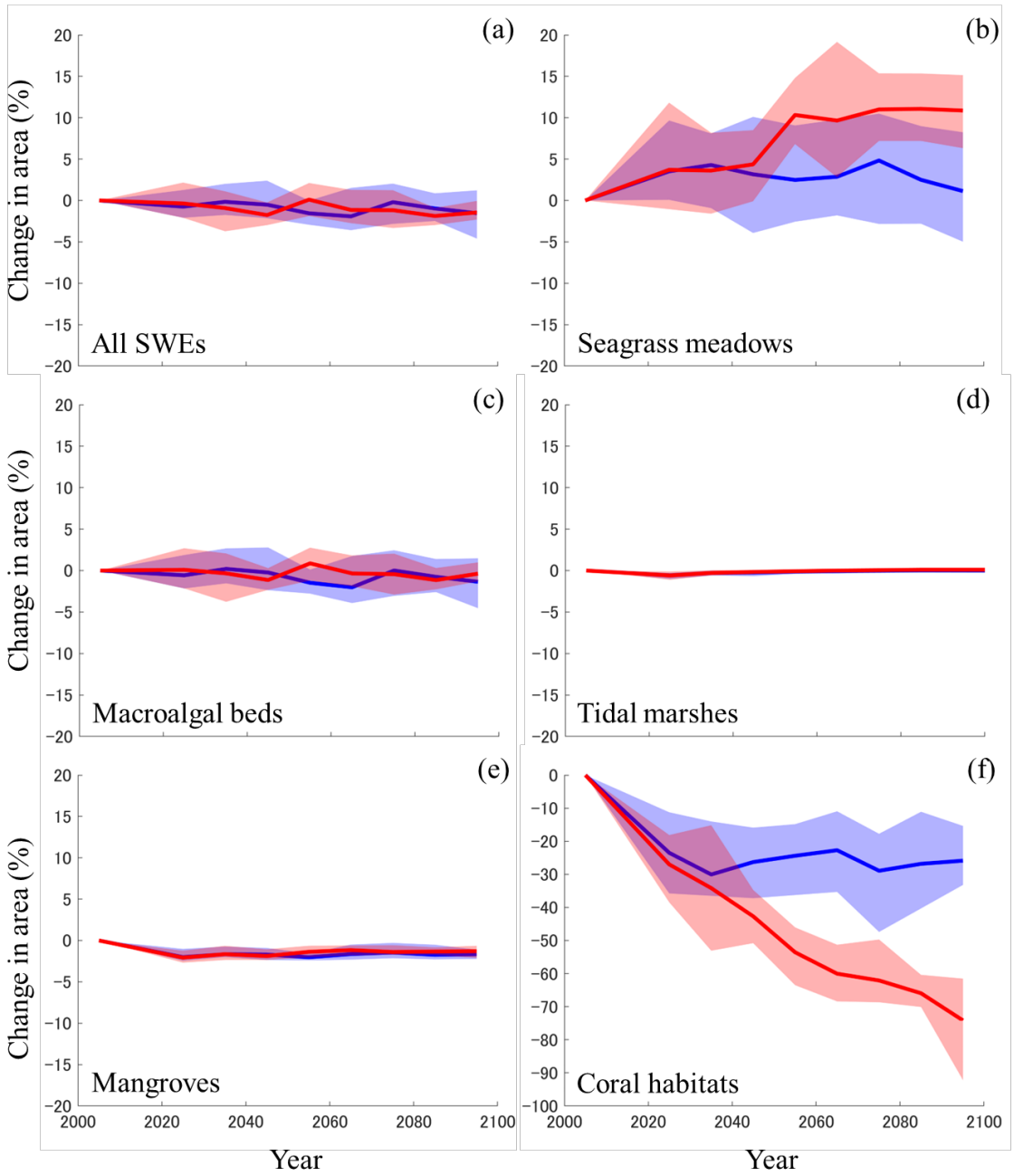

Figure 1. Changes in global areas of shallow water ecosystems (SWEs) relative to the present. a All SWEs, b seagrass meadows, c macroalgal beds, d tidal marshes, e mangroves, f coral habitats. Blue lines are for RCP2.6 and red lines are for RCP8.5. Shading indicates ranges between minimal and maximal values

during each calendar decade (Table S2).

Table 1. Areas of SWEs in present and projected future conditions.

	Present	2050s	2090s		
		RCP2.6	RCP8.5	RCP2.6	RCP8.5
Seagrass meadows	308,610 (7.5)	316,269 (7.8)	340,494 (8.2)	312,109 (7.7)	342,162 (8.4)
Macroalgal beds	3,510,000 (84.9)	3,458,320 (85.1)	3,540,415 (85.6)	3,462,541 (85.3)	3,496,730 (85.8
Tidal marshes	54,706 (1.3)	54,638 (1.3)	54,663 (1.3)	54,701 (1.3)	54,763 (1.3)
Mangroves	153,690 (3.7)	150,575 (3.7)	151,586 (3.7)	151,134 (3.7)	151,697 (3.7)
Coral habitat	108,314 (2.6)	81,898 (2.0)	50,285 (1.2)	80,290 (2.0)	27,984 (0.7)

Note: Areas are in km^2; percentages of the area of each of the five global SWEs are in parentheses.

3.1 Seagrass meadows and macroalgal beds

The area of seagrass meadows was projected to be stable in RCP2.6, but increase by 11% in RCP8.5, from the present to 2100 (Figure 1b). By region, seagrass meadows were predicted to expand the most in East-South Africa and West Africa and to shrink the most in the Mediterranean (Tables S7 and S8). The projected extent of macroalgal beds before 2100 varied within a narrow range from 2% to 0.9% (Figure 1c).

The difference in the area change of seagrass meadow between the two RCP scenarios is due to the photosynthetic active radiation depth (Z_c), which was close to the current value in RCP2.6 (around 22 m) but slightly deeper in RCP8.5 (23 m) by 2100 because of a continuing decrease in the chlorophyll concentration (Figure S7). The future Z_c varied between 21 and 23 m (for seagrass meadows) and 62 and 66 m (for macroalgal beds) and became slightly deeper starting around 2050 in RCP8.5. The maximal differences in Z_c between the two RCP scenarios were about 1.6 m in seagrass meadows and about 3.7 m in macroalgal beds. The decrease in chlorophyll concentrations can be accelerated by reduced nutrient supplies as upwelling weakens under global warming (Gregg et al., 2005). As a result, the transparency of sea water increases, and the expansion of favorable habitat for seagrass meadows and macroalgal beds may be particularly noticeable in RCP8.5.

Our results showing a 11% extension of seagrass meadows by 2100 contrast with a previous study showing a decrease of 8.6% in RCP8.5 (Jorda et al., 2020). This discrepancy may reflect a difference between in the assumed changes in the euphotic layer. The previous study assumed a constant euphotic layer depth, whereas this study assumed that changes in chlorophyll concentration would

deepen the euphotic layer. If our model assumes no change in chlorophyll concentration (and thus no change in euphotic layer depth), the extent of seagrass meadows would decrease by 2.5% from the present (Figure S8), similar to the previous study. However, the assumption of no sea-level changes permits the extent of seagrass meadows to expand 8.9% by 2100. Therefore, it appears that the future change in the euphotic layer can have significant impacts on seagrass meadow habitat.

Our results showing almost no change in the area of macroalgal beds (2% to 0.9%) by 2100 also differ markedly from the previous study, which predicted a decrease of kelp (seaweeds belonging to Laminariaceae) by 20.6% in the RCP8.5 scenario (Jorda et al., 2020). First, we considered all groups of macroalgae, whereas the previous study considered only the kelp group. Second, while the previous study set upper water temperature limit of 26°C for predicting sustainable kelp habitats (Jorda et al., 2020), our study ignored water temperature because each macroalgal group has different optimal water temperatures (Eggert, 2012); thus, even if changing water temperature induces a shift in macroalgae species, the distribution changes for the whole macroalgal group are unpredictable given current knowledge. For this reason, comparisons with the previous study are problematic.

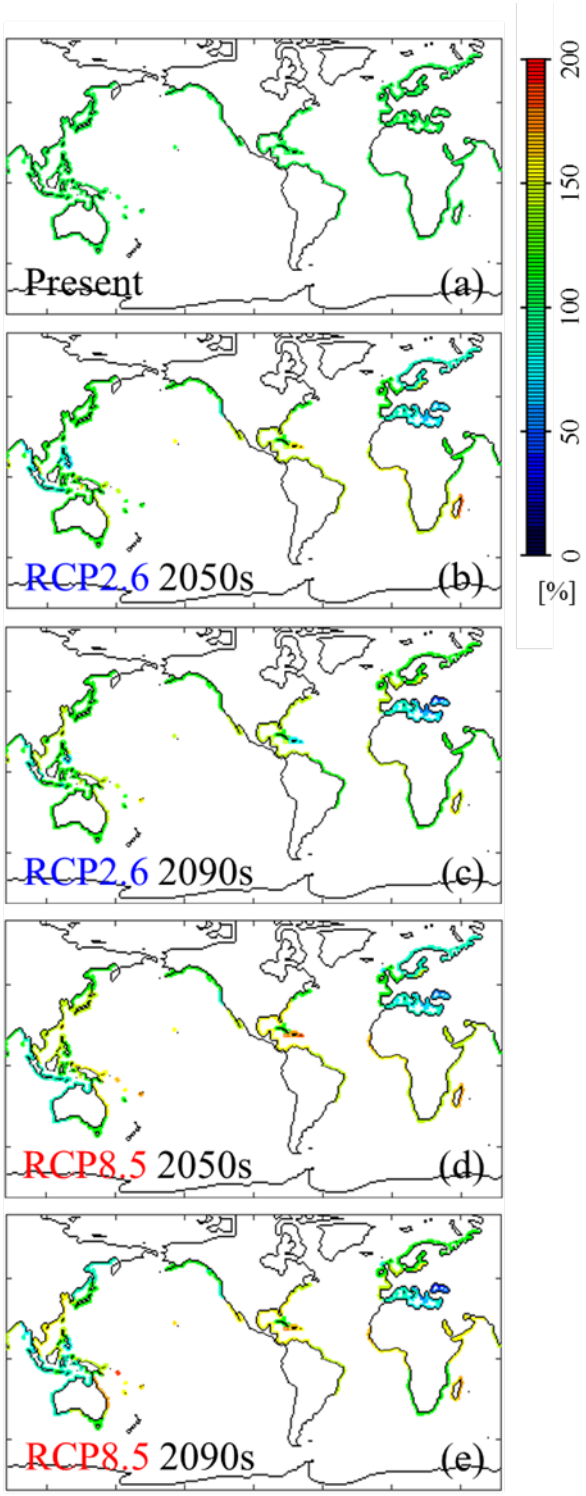
Present
(a)
RCP2.6 2050s
(b)
RCP2.6 2090s
(c)
RCP8.5 2050s
(d)
RCP8.5 2090s
(e)
200
150
100
50
0
[%]

Figure 2. Predicted global distribution of seagrass meadows. a Present, b 2050s in RCP2.6, c 2090s in RCP2.6, d 2050s in RCP8.5, e 2090s in RCP8.5. The color bar shows changes in area; the present area is 100%.

3.2 Tidasl marshes and mangroves

The areas of tidal marshes and mangroves were projected to be almost stable in both RCP scenarios by 2100 (Figure 1d and 1e). Our results showed that the areas of these SWEs did not change under sea-level change.

The area of tidal marshes was projected to continuously expand in the Black Sea (in the Mediterranean region) in the both RCP scenarios, while the projected distribution was almost stable between the RCP scenarios in other regions (Figure 3a–e and Tables S7 and S8). These spatial differences can be attributed to regional differences in sea-level change and the relationship between sea-level change and the topographic gradient in the cross-shore direction. These details are discussed below.

In both RCP scenarios, the projected distribution area of mangroves also showed no marked differences from the present (Figure 3f–j, Tables S7 and S8).

Future sea-level change in the global coastal regions is presented in Figure S9. In both RCP scenarios, average sea-level changes in each computational region by 2100 were 0.2 m in RCP2.6 and 0.4 m in RCP8.5. The range of sea-level changes in the 2090s was between 0.3 m and 0.2 m in RCP2.6 (difference: 0.5 m) and between 0.6 m and 0.3 m in RCP8.5 (difference: 0.9 m). Although sea level is rising as a global average due to climate change, sea level can locally fall because of changes in ocean currents (Church et al., 2013). Thus, changes in the area of SWEs are dependent on sea-level change in each region.

Consequently, the relationship between geomorphic gradients and sea level determines the future change in the area of tidal marshes and mangroves (Figure 4 and Figure S10). If sea-level rise occurs in areas where slopes grow gentler away from the shoreline, tidal marshes and mangroves in the intertidal zone will expand into more area than is lost (Figure 4a and 4b). In turn, when the sea level falls, the area lost is greater than the area expanded (Figure S10a and S10b). If the landward slope is steeper than the seaward slope, sea-level rise reduces more area than it expands (Figure 4d and 4e); the opposite is true when sea level falls (Figure S10c and S10d).

Our results from tidal marshes and mangroves differ greatly from those of SROCC (IPCC, 2019), which projected that coastal wetlands (tidal marshes, mangroves, and seagrass meadows) will shrink by 20 90% from present conditions (Blankespoor et al., 2014; Crosby et al., 2016; Spencer et al., 2016). Although direct comparisons of the two studies are difficult, the reason for this discrepancy may be that SROCC assumed 1 m of sea-level rise by 2100 (Blankespoor et al., 2014), which is an overestimate compared to the average value of RCP8.5, but the studies also differ in other data used. However, if sea-level rise is set at 1 m in our model, then the area of tidal marshes is stable (Figure

S11a) and that of mangroves expands by 3.5% (Figure S11b), respectively. Additionally, we carried out a numerical prediction in order to assess the effects of the landward shift of SWEs relative to sea-level rise. This projection assumed that the landward shift of SWEs relative to sea-level rise was limited due to the presence of global coastal hard infrastructures and land use (Figure 4c and 4f). Our projection showed that 91.9% of tidal marshes and 74.3% of mangroves are lost by 2100 in RCP8.5 (Figure 5). Similarly, Kirwan et al. (Kirwan et al., 2010) and Lovelock et al. (2015) showed that SWE areas shrank considerably due to sea-level rise (similar to Figure 5) because coastal structures were assumed to exist. In addition, they predicted that sedimentation prevented SWE shrinkage despite the fact the SWEs could not shift landward because the seafloor rise by sedimentation offset the effects of the sea-level rise. In this study, sedimentation was not considered in tidal marshes and mangroves, although the results showed that the area will at least be sustained if a landward shift of SWEs is allowed. Sedimentation does not necessarily follow sea-level rise, and it has also been shown that the self weight can accelerate subsidence discussed below (Saintilan et al., 2022). Therefore, the future sustainability of tidal marshes and mangroves as the sea-level rises depends on whether SWEs can shift landward. These points support the view that the projections from our model are an improvement over those of previous studies. However, there are still large gaps in these future projections. Hard coastal structures (e.g., seawalls) and related land use (e.g., culture ponds) are distributed along the coasts of many countries (e.g., hard infrastructure covers 14% of the U.S. coastline (Gittman et al., 2015)), but global data on these subjects are inadequate for the present and nonexistent for future projections.

There are also regions where sea level falls, but the effects of the disappearance of tidal marshes and mangroves are considerably less than those caused by sea-level rise (Figure S12). Furthermore, our model considers globally calculated sea-level change as an external forcing, but discrepancies can be created if local sea-level change based on observed data is applied (Crosby et al, 2016).

SWEs such as tidal marshes and mangroves distributed in coastline areas can be influenced not only by sea-level rise but also by subsidence. Because subsidence in several deltas in the world has been reported (Syvitski et al., 2009), this study also estimated the effects of subsidence to SWEs in the corresponding model regions (Tables S5 and S6). In most of the regions, the distribution was not changed even when subsidence was taken into account, but the distribution was predicted to significantly expand in Thailand, Vietnam and China (Label 82). Mangroves additionally expand in India and Bangladesh (Label 14) and Pakistan (Label 32). In particular, our model showed that the distributions of tidal marshes and mangroves expands by almost 3.2 times and 3.7 times current levels, respectively, in Thailand, Vietnam and China. It is assumed that tidal marshes and mangroves inhabit the intertidal zone on land side at the present; therefore, the expansion area offsets the disappearing area by moving landward with sea-level rise. However, as the SWEs shift toward the gentler landward slope with sea-level rise, which was relatively increased by subsidence, the ar-

eas expanded markedly (Figure 4b). Conversely, despite the large subsidence, due to sea-level rise by 2100 (Figure S9), the area of SWEs did not markedly expand because the topographic gradient becomes steeper in a landward direction (Figure 4e). Thus, differences in SWE distribution between the regions can be great if subsidence significantly differs in each region. The subsidence data, however, contain much uncertainty, are generally lacking, and have a coarse spatial resolution (Minderhoud et al, 2019).

If SWEs expand landward relative to sea-level rise, sea-side SWEs necessarily shrink. If subsidence also occurs in a region where sea-level rise occurs, such shrinkage can be accelerated. Thus, it is very important to include such shrinkage when making predictions of various hazards and considering countermeasures.

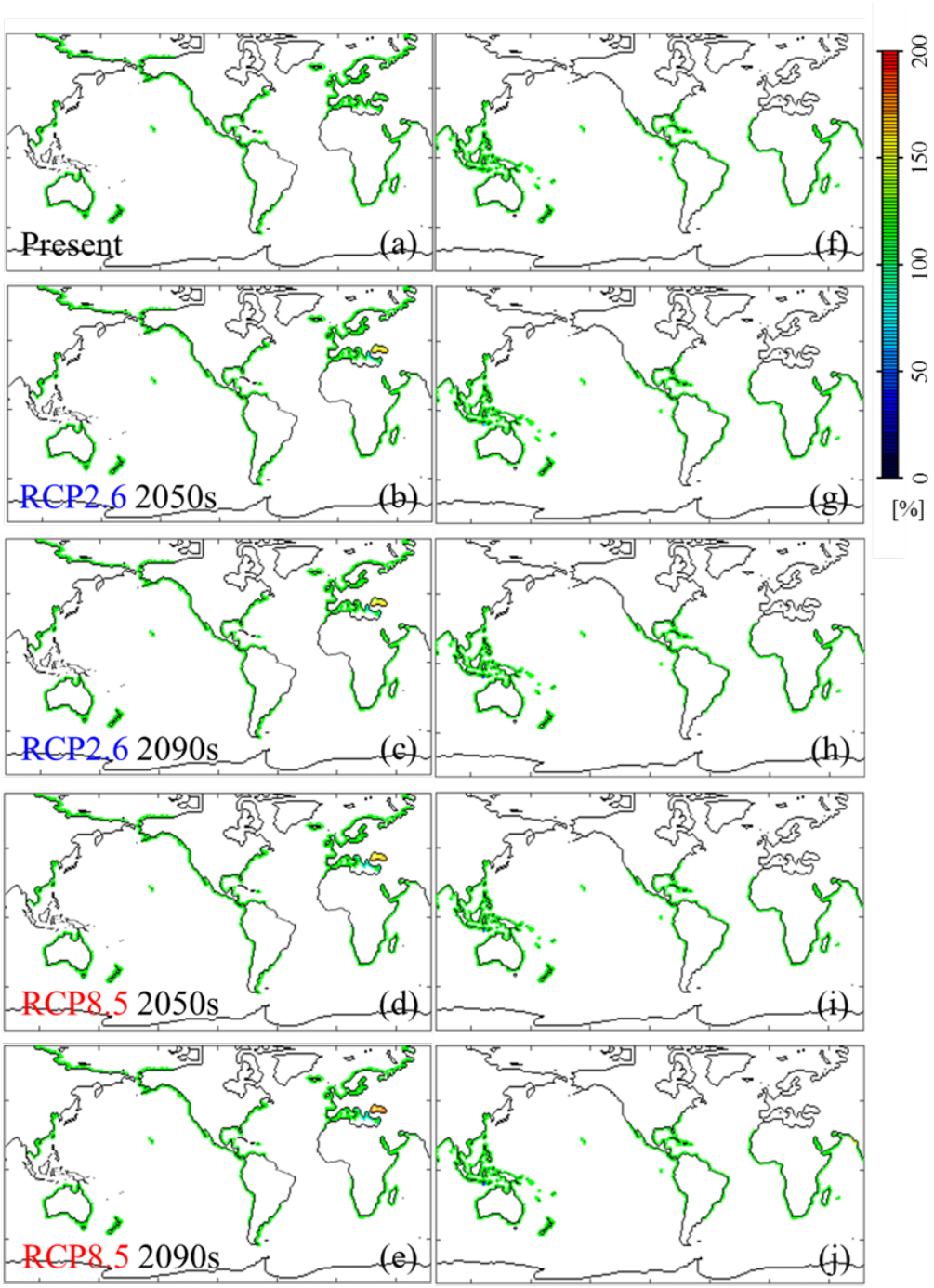

Figure 3. Predicted global distribution of tidal marshes and mangroves. a

Tidal marshes in the present, b 2050s in RCP2.6, c 2090s in RCP2.6, d 2050s in RCP8.5, e 2090s in RCP8.5. f Mangroves in the present, g 2050s in RCP2.6, h 2090s in RCP2.6, i 2050s in RCP8.5, j 2090s in RCP8.5. The color bar shows changes in area; the present area is 100%.

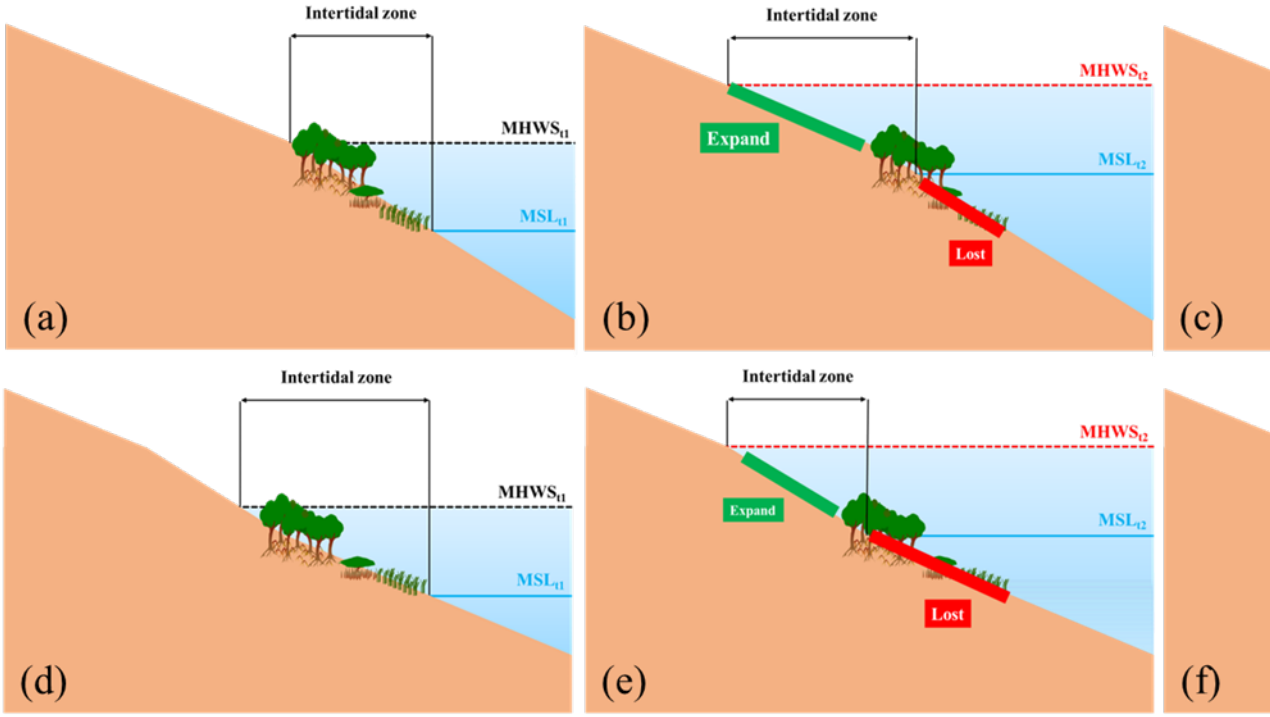

Figure 4. Hypsometric relations between sea-level rise and area of SWEs. Schematic views of the relationship between geomorphic slope where a the landward slope is gentler than the seaward slope and the resulting SWE changes under sea-level rise in a coastal setting b without hard infrastructure and c with hard infrastructure, and where d the landward slope is steeper than the seaward slope and the resulting SWE changes under sea-level rise e without hard infrastructure and f with hard infrastructure. MSL_{t1}, present mean sea level; $MHWS_{t1}$, present mean high water spring tide level; MSL_{t2}, future mean sea level; $MHWS_{t2}$, future mean high water spring tide.

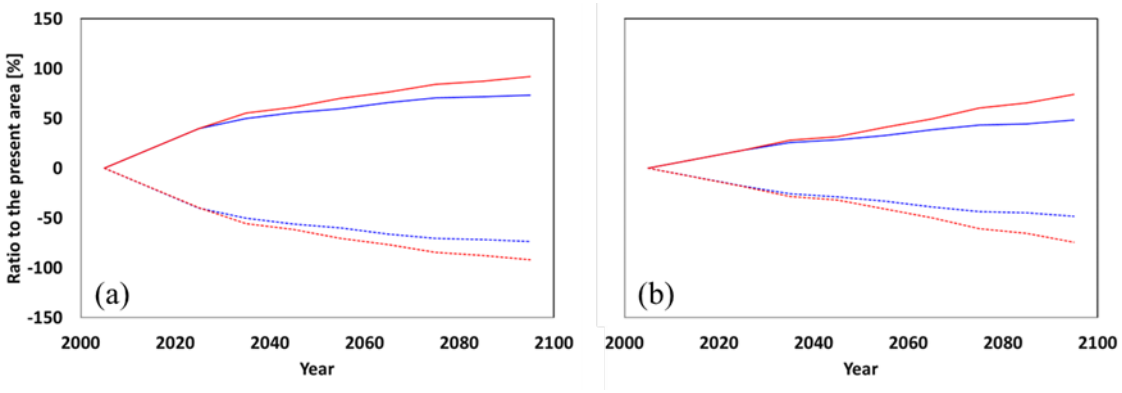

Figure 5. SWE areas gained and lost with sea-level rise. Shown are percentages relative to the present of area lost (dashed line) and gained (solid line) in habitat for a tidal marshes and b mangroves due to sea-level rise. Blue and red colors represent changes in RCP2.6 and RCP8.5, respectively.

3.3 Coral habitats

Our projections showed that 30% of global coral habitats disappeared in RCP2.6 and RCP8.5 by the 2030s (Figure 1f). They expanded slightly in RCP2.6 after the 2030s, but 26% disappeared by 2100. In RCP8.5, coral habitats continued to decrease after the 2030s, and 74% was gone by 2100. A key threshold for coral habitat is the sea surface temperature (SST) during the warmest month of the year, as coral bleaching begins at 30°C. In RCP2.6, SST was largely unchanged, and more than half of the global coral habitat lay below 30°C (Figure S13). In RCP8.5, SST continued to increase in all areas until 2100, and it was projected to exceed the 30°C threshold in more than half of the area by the 2050s.

By region, our results showed that coral habitats were significantly affected in lower latitudes, particularly in southeast Asia (Figure 6 and Tables S7 and S8). Coral habitat was projected to rise only in the Mediterranean by 2100 in RCP8.5.

Although Frieler et al. (2013) predicted greater habitat loss than we did, our results are similar to those of Jorda et al. (2020). Jorda et al. (2020) adopted a water temperature with an upper limit of 30°C, similar to the procedure used in our model, whereas Frieler et al. (2013) applied the degree heating month, which is the integral of the difference between the monthly mean SST and the reference warmest month SST. Thus, the gap between these projections may be caused by the difference in methods used, but the studies all project that coral habitats will shrink significantly in the future, so countermeasures that focus on ecosystem services and other factors may be necessary.

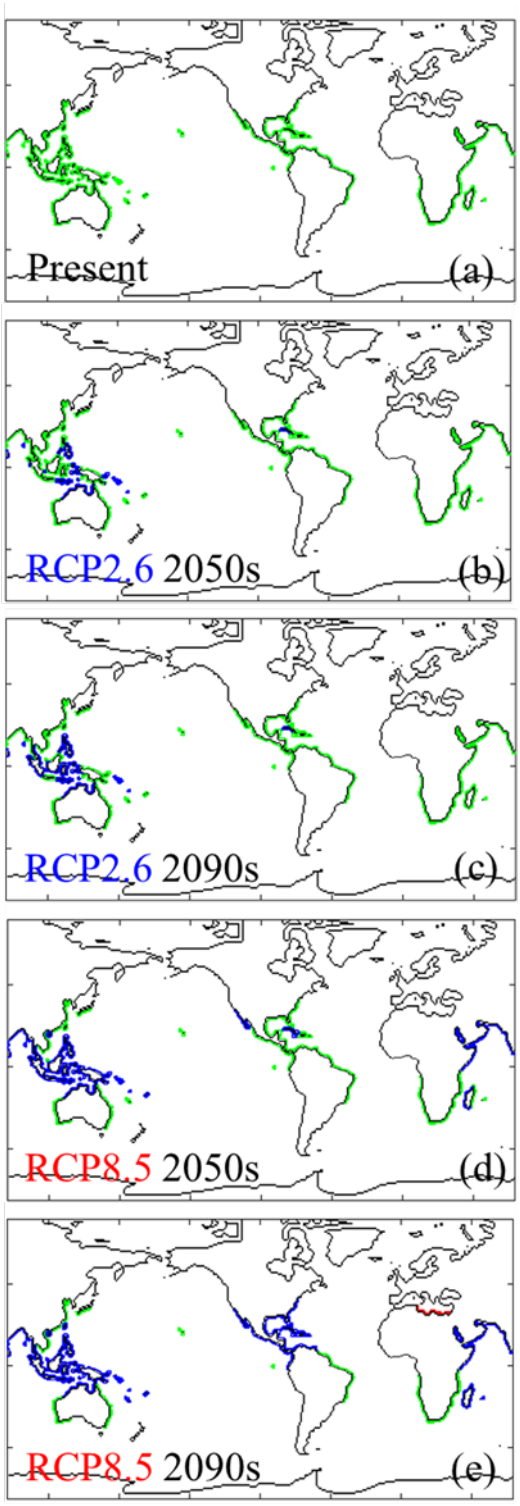
Present
(a)
RCP2.6 2050s
(b)
RCP2.6 2090s
(c)
RCP8.5 2050s
(d)
RCP8.5 2090s
(e)

Figure 6. Projected global distribution of coral habitat. a Present, b 2050s in RCP2.6, c 2090s in RCP2.6, d 2050s in RCP8.5, e 2090s in RCP8.5. Green, blue and red represent areas of no change, loss due to climate change and expansion due to climate change, respectively.

5 Conclusions

Coral habitats shrank by 74% by 2100 under RCP8.5, but macroalgal beds, tidal marshes, and mangroves were sustainable and seagrass meadows expanded by 11%. If coastal development such as hard infrastructure and land use is assumed, however, tidal marshes and mangroves shrank by 91.9% and 74.3%, respectively.

Because of the potential for considerable loss of coral reefs, which are effective in wave attenuation, it may be necessary to consider countermeasures that include the best mix of coastal hard infrastructure and SWEs reduce coastal hazards in the future. Sustaining or expanding the distribution of the other SWEs, which have relatively high CO_2 absorption (Kuwae and Hori, 2019), with appropriate coastal management is a promising avenue for climate change mitigation.

Acknowledgments

We thank Dr. Hiroya Yamano and Dr. Tomomi Inoue of the National Institute for Environmental Studies for their advice and assistance with the use of topographical data and ecosystem distribution data. Dr. Yamano also advised us on the prediction of changes in coral habitat area. Mr. Taichi Kosako of the Port and Airport Research Institute provided guidance and advice on data analysis of GCM and TPXO.

This work was partly supported by the Environmental Research and Technology Development Fund (S-14: JPMEERF15S11408) of the Environmental Restoration and Conservation Agency of Japan, and Grants-in-Aid for Scientific Research (KAKENHI) from the Japan Society for the Promotion of Science (nos. 18H04156 and 26630251).

Competing Interest Statement: Authors Keigo Yanagita and Keiichi Kondo were employed by the company Science and Technology Co., LTD. All other authors declare no competing interests.

References

Arin, L., Guillen, J., Segura-Noguera, M., & Estrada, M. (2013). Open sea hydrographic forcing of nutrient and phytoplankton dynamics in a Mediterranean coastal ecosystem. *Estuarine, Coastal and Shelf Science*, 133, 116-128, doi:10.1016/j.ecss.2013.08/018.

Assis, J., Fragkopoulou, E., Frade, D., Neiva, J., Oliveira, A., Abecasis, D., … Serrao, A. E. (2020). A fine-tuned global distribution dataset of marine forests. *Scientific Data*, 7 (1), 1-9, doi:10.1038/s41597-020-0459-x.

Blankespoor, B., Dasgupta, S., & Laplante, B. (2014). Sea-level rise and coastal wetlands. *Ambio*, 43 (8), 996-1005, doi:10.1007/s13280-014-0500-4.

Borum, J., & Sand-Jensen, K. (1996). Is total primary production in shallow coastal marine waters stimulated by nitrogen loading?. *Oikos*, 76, 406-410, doi:10.2307/3546213.

Bouma, T. J., van Duren, A. L., Temmerman, S., Claverie, T., Blanco-Garcia, A., Ysebaert, T., & Herman, J. M. P. (2007). Spatial flow and sedimentation patterns within patches of epibenthic structures: Combining field, flume, and modelling experiments. *Continental Shelf Research*, 27, 1020-1045, doi:10.1016/j.csr.2005.12.019.

Church, J. A., Clark, P. U., Cazenave, A., Gregory, J. M., Jevrejeva, S., Levermann, A., … Unnikrishnan, A. A. (2013). *Sea level change*, Cambridge, UK, PM Cambridge University Press.

Crosby C. S., Sax, F. D., Palmer, E. M., Boothe, S. H., Deegan, A. L., Bertness, D. M., & Leslie, M. H. (2016). Salt marsh persistence is threatened by predicted sea-level rise. *Estuarine, Coastal and Shelf Science*, 181, 93-99, doi:http://dx.doi.org/10.1016/j.ecss.2016.08.018.

Delesalle, B., Pichon, M., Frankignoulle, M., & Gattuso, J. P. (1993). Effects of a cyclone on coral reef phytoplankton biomass, primary production and composition (Moorea Island, French Polynesia). *Journal of Plankton Research*, 15 (12), 1413-1423, doi:10.1093/plankt/15.12.1413.

Dennison, W. C. (1987). Effects of light on seagrass photosynthesis, growth and depth distribution. *Aquatic Botany*, 27 (1), 15-26, doi:10.1016/0304-3770(87)90083-0.

Duarte, M. C. (1991). Seagrass depth limits. *Aquatic Botany*, 40, 363-377.

Duarte, M. C., Middelburg, J. J., & Caraco, N. (2005). Major role of marine vegetation on the oceanic carbon cycle. *Biogeosciences*, 1, 659-679, doi:10.5194/bg-2-1-2005.

Duarte M. C., Losada, J. I., Hendriks, E. I., Mazarrasa, I., & Marba, N. (2013). The Role of Coastal Plant Communities for Climate Change Mitigation and Adaptation. *Nature Climate. Change*, 3, 961-968, doi:10.1038/nclimate1970.

Duarte, M. C., Agusti, S., Barbier, E., Britten, L. B., Castilla. C. J., Gattuso, J-P., … Worm, B. (2020). Rebuilding Marine Life. *Nature*, 580, 39-51 (2020), doi:10.1038/s41586-020-2146-7.

Dunne, P. J., John, G. J., Adcroft, J. A., Griffies, M. S., Hallberg, W. R., Shevliakova, E., … Zadeh, N. (2012). GFDL's ESM2 global coupled climate-carbon earth system model. Part I: Physical formulation and baseline simulation characteristics. *Journal of Climate*, 25, 6646-6665, doi:10.1175/JCLI-D-11-00560.1.

Durr, H. H., Laruelle, G. G., van Kempen, M. C., Slomp, P. C., Meybeck, M., & Middelkoop, H. (2011). Worldwide typology of nearshore coastal systems:

Defining the estuarine filter of river inputs to the oceans. *Estuaries and Coasts*, 34, 441-458, doi:10.1007/s12237-011-9381-y.

Egbert, G. D., & Erofeeva, S. Y. (2002). Efficient inverse modeling of barotropic ocean tides. *Journal of Atmospheric and Oceanic Technology*, 19, 183-204, doi:10.1175/1520-0426(2002)019<0183:EIMOBO>2.0.CO;2.

Eggert, A. (2012). Seaweed response to temperature. In C. Wienche, K. Bischof (Eds.), *Seaweed Biology* (pp. 47-66). Heidelberg, Springer, doi:10.1007/978-3-642-28451-9.

Frieler, K., Meinshausen, M., Golly, A., Mengel, M., Lebek, K., Donner, D. S., & Hoegh-Guldberg, O. (2013). Limiting global warming to 2 ℃ is unlikely to save most coral reefs. *Nature Climate Change*, 3, 165-170, doi:10.1038/nclimate1674.

Gattuso, P-J., Gentili, B., Duarte, M. C., Kleypas, A. J., Middelburg, J. J., & Antoine, D. (2006). Light availability in the coastal ocean: impact on the distribution of benthic photosynthetic organisms and contribution to primary production. *Biogeosciences Discussions*, 3, 895-959.

Gittman, R. K., Fodrie, J. F., Popowich, M. A., Keller, A. D., Bruno, F. J., Currin, A. C., … Piehler, F. M. (2015). Engineering away our natural defenses: an analysis of shoreline hardening in the US. *Frontiers in Ecology and the Environment*, 13 (6), 301-307, doi:10.1890/150065.

Gregg, W. W., Casey, N. W., & McClain, C. R. (2005). Recent trends in global ocean chlorophyll. *Geophysical Research Letters*, 32 (3), doi:10.1029/2004GL021808.

Guinotte, J. M., Buddemeier, R. W., & Kleypas, J. A. (2003). Future coral reef habitat marginality: temporal and spatial effects of climate change in the Pacific basin. *Coral Reefs*, 22, 551-558, doi:10.1007/s00338-003-0331-4.

Haight, C., Larson, M., Swadek, R. K. & Hartig, E. K. (2019). Toward a Salt Marsh Management Plan for New York City: Recommendations for Strategic Restoration and Protection. *Coastal Wetlands*, 997-1022 (2019).

Hanelt, D., & Figueroa, L. F. (2012). Physiological and photomorphogenic effects of light on marine macrophytes. In C. Wienche, & K. Bischof (Eds.), *Seaweed Biology* (pp. 3-24). Heidelberg, Springer, doi:10.1007/978-3-642-28451-9.

Harrison, J. P., & Hurd, L. C. (2001). Nutrient physiology of seaweeds: Application of concepts to aquaculture. *Cahiers de Biologie Marine*, 42, 71-82.

Hoegh-Guldberg, O., & Smith, G. J. (1989). The effect of sudden changes in temperature, light and salinity on the population-density and export of zooxanthellae from the reef corals Stylophora pistillata Esper and Seriatopora hystrix Dana. *Journal of Experimental Marine Biology and Ecology*, 129, 279-303, doi:10.1016/0022-0981(89)90109-3.

Hori, M., Bayne, J. C., & Kuwae, T. (2019). *Blue Carbon: Characteristics of the Ocean's Sequestration and Storage Ability of Carbon Dioxide.* Beach Road, Singapore, Kuwae, T., & Hori, M. (2019). *Blue carbon in shallow coastal ecosystems: carbon dynamics, policy, and implementation.* Springer Nature, pp. 1-32. doi:10.1007/978-981-13-1295-3.

IPCC. (2019). *Special report on the ocean and cryosphere in a changing climate (SROCC).* https://www.ipcc.ch/srocc/home/.

Jickells, T. D. (1988). Nutrient biogeochemistry of the coastal zone. *Science*, 281 (5374), 217-222, doi:10.1126/science.281.5374.217.

Jorda, G., Marba, N., Bennett, S., Santana-Garcon, J., Agusti, S., & Duarte, M. C. (2020). Ocean warming compresses the three-dimensional habitat of marine life. *Nature Ecology & Evolution*, 4, 109-114, doi:10.1038/s41559-019-1058-0.

Kay, R., & Wilderspin, I. (2002). Box 4.4: Mangrove Planting Saves Lives and Money in Viet Nam. *World Disaster Report Focus on Reducing Risk*, 95, Geneva: International Federation of The Red Cross and Red Crescent Societies (IFRCRCS).

Kayanne, H., Harii, S., Yamano, H., Tamura, M., Ide, Y., & Akimoto, F. (1999). Changes in living coral coverage before and after the 1998 bleaching event on coral reef flats of Ishigaki Island, Ryukyu Islands. *Journal of the Japanese Coral Reef Society*, 1, 73-82, doi:10.3755/jcrs.1999.73 (in Japanese with English abstract).

Kirwan, L. M., Guntenspergen, R. G., D'Alpaos, A., Morris, T. J., Mudd, M. S. & Temmerman, S. (2010). Limits on the adaptability of coastal marshes to rising sea level. *Geophysical. Research. Letters,* 37, doi:10.1029/2010GL045489.

Kirwan, M. L., & Mudd, S. M. (2012). Response of Salt-marsh Carbon Accumulation to Climate Change. *Nature*, 489, 550-553, doi:10.1038/nature11440.

Kleypas, J. A., Buddemeier, W. R., Archer, D., Gattuso, J-P., Langdon, C., & Opdyke, N. B. (1999). Geochemical consequences of increased atmospheric carbon dioxide on coral reefs. *Science*, 234, 118-120, doi:10.1126/science.284.5411.118.

Krause-Jensen, D., & Duarte, M. C. (2016). Substantial of macroalgae in marine carbon sequestration. *Nature Geoscience*, 9 (10), 737-742, doi:10.1038/NGEO2790.

Kuwae, T., & Hori, M. (2019). The Future of Blue Carbon: Addressing Global Environmental Issues. In T. Kuwae & M. Hori (Eds.), *Blue carbon in shallow coastal ecosystems: carbon dynamics, policy, and implementation* (pp. 322-347). Beach Road, Singapore, Springer Nature, doi:10.1007/978-981-13-1295-3.

Lee, S-K., Park, R. S., & Kim, K. Y. (2007). Effects of irradiance, temperature, and nutrients on growth dynamics of seagrasses: A review. *Journal of Experimental Marine Biology and Ecology*, 350, 144-175,

doi:10.1016/j.jembe.2007.06.016.

Lovelock, E. C., Cahoon, R. D., Friess, A. D., Guntenspergen, R. G., Krauss, W. K., Reef, R., … Triet, T. (2015). The vulnerability of Indo-Pacific mangrove forests to sea-level rise. *Nature*, 526, 559-563, doi:10.1038/nature15538.

Lovelock,E. C., & Reef, R. (2020). Variable impacts of climate change on blue carbon. *One Earth*, 3, 195-211, doi:10.1016/j.oneear.2020.07.010.

Minderhoud, P. S. J., Coumou, L., Erkens, G., Middelkoop, H., & Stouthamer, E. (2019). Mekong delta much lower than previously assumed in sea-level rise impact assessments. *Nature Communications*, 10 (1), 1-13, doi:10.1038/s41467-019-11602-1.

Morel, A. (1988). Optical modelling of the upper ocean in relation to its biogenous matter content (Case 1 waters). *Journal of Geophysical Research*, 193 (C9), 10749-10768, doi:10.1029/JC093iC09p10749.

Nellman, C., Corcoran, E., Duarte, M. C., Valdes, L., De Young, C., Fonseca, L., & Grimsditch, G. (2009). *Blue carbon. A rapid response assessment.* Birkeland Tryckeri As, Birkeland, United Nations Environmental Programme, GRID-Arendal.

Nielsen, S. L., Sand-Jensen, K., Borum, J., & Geertz-Hansen, O. (2002). Depth colonization of eelgrass (Zostera marina) and macroalgae as determined by water transparency in Danish coastal waters. *Estuaries*, 25, 1025-1032, doi:10.1007/BF02691349.

Nuttle, W., Brinson, M., & Cahoon, C. (1997). Processes that maintain coastal wetlands in spite of rising sea level. *Eos (Transactions American Geophysical Union)*, 78 (25), 257-261 (1997).

Phan, L. K., van Thiel de Vries, J. S., & Stive, M. J. (2015). Coastal mangrove squeeze in the Mekong delta. *Journal of Coastal Research*, 31 (2), 233-243, doi:10.2112JCOASTRES-D-14-00049.1.

Saintilan, N., Kovalenko, E. K., Guntenspergen, G., Rogers, K., Lynch, C. J., Cahoon, R. D., … N. Khan. (2022). Constraints on the adjustment of tidal marshes to accelerating sea level rise. *Science*, 377, 523-527, doi:10.1126/science.abo7872.

Schuerch, M., Spencer, T., Temmerman, S., Kirwan, L. M., Wolff, C., Lincke, D. … Brown, S. (2019). Future response of global coastal wetlands to sea-level rise. *Nature*, 561, 231-234, doi:10.1038/s41586-018-0476-5.

Spencer, T., Scherch, M., Nicholls, J. R., Hinkel, J., Lincke, D., Vafeidis, T. A., … Brown, S. (2016), Global coastal wetland change under sea-level rise and related stresses: The DIVA Wetland Change Model. *Global and Planetary Change*, 139, 15-30, doi:https://doi.org/10.1016/j.gloplacha.2015.12.018.

Struve, J., Falconer, R. A., & Wu, Y. (2003). Influence of model mangrove trees on the hydrodynamics in a flume. *Estuarine, Coastal. and Shelf Science*, 58 (1),

163-171, doi:10.1016/S0272-7714(03)00072-6.

Syvitski, J. P., Kettner, J. A., Overeem, I., Hutton, H. W. E., Hannon, T. M., Robert, G., … Nicholls, J. R. (2009). Sinking deltas due to human activities. *Nature Geoscience*, 2 (10), 681, doi:10.1038/NGEO629.

Takao, S., Kumagai, H. N., Yamano, H., Fujii, M., & Yamanaka, Y. (2015). Projecting the impacts of rising seawater temperatures on the distribution of seaweeds around Japan under multiple climate change scenarios. *Ecology and Evolution*, 5 (1), 213-223, doi:10.1002/ece3.1358.

Taylor, K. E., Stouffer, R. J., & Meehl, G. A. (2012). An overview of CMIP5 and the experiment design. *Bulletin of the American Meteorological Society*, 93 (4), 485-498, doi:10.1175/BAMS-D-11-00094.1.

Ward, G. L., Kepm, M. W., & Boynton, R. W. (1984). The influence of waves and seagrass communities on suspended particulates in an estuarine embayment. *Marine Geology*, 59, 85-103, doi:10.1016/0025-3227(84)90089-6.

Yara, Y., Vogt, M., Fujii, M., Yamano, H., Hauri, C., Steinacher, M., … Yamanaka, Y. (2012). Ocean acidification limits temperature-induced poleward expansion of coral habitats around Japan. *Biogeosciences*, 9, 4955-4968, doi:10.5194/bg-9-4955-2012.